Ionization of glucose and ribose molecules by electron impact

Sándor Demes, A. Zavilopulo, E. Remeta

Preprint 10 October 2023

Ionization of glucose and ribose molecules by electron impact

S. Demes[1b], A. Zavilopulo[2a], E. Remeta[2c]

[1]Institute for Nuclear Research (ATOMKI), 18/C Bem square Debrecen 4026, Hungary
[2]Institute of Electron Physics, National Academy of Sciences of Ukraine, 21 Universitetska str., 88017 Uzhhorod, Ukraine

Abstract. The ionization potentials and total ionization cross sections of glucose and ribose monosaccharide molecules were measured by electron impact at energies up to 70 eV. Using two methods, Hartree-Fock (HF) and density functional theory (DFT), the structure of D- and L-forms of glucose and ribose molecules were calculated using Gaussian. The energy characteristics of the molecular orbitals (MOs) were used to calculate the summarized single ionization cross sections (CS) based on the MOs by the Binary-Encounter-Bethe (BEB) and Gryzinsky (Gryz) models. By normalizing to Gryz-DFT cross sections at thresholds, at 11 eV (Glucose) and 12.65 eV (Ribose), the absolute values of the measured total ionization cross sections of these molecules were obtained. The ionization potentials of glucose and ribose molecules were evaluated from binding HOMO MOs energies and compared with the measured values: 12.25 ± 0.25 eV (Glucose) and 10.46 ± 0.25 eV (Ribose). The contributions of the higher orbitals HOMO, HOMO-1, HOMO-2 to the Gryz-DFT cross section were evaluated.

This is a preprint article. The VOR is available online at: 10.1140/epjd/s10053-023-00766-7

1 Introduction

The biological significance of monosaccharides stimulates their studies due to electronic interactions. Understanding the mechanisms of energy dissipation in organic and biomolecules is extremely important both for studying processes occurring in living organisms and for studying radiation damage of biological matter. Interaction of ionizing radiation with a living organism can cause various genotype changes by affecting DNA and RNA macromolecules. Penetrating the body, radiation generates a flow of low-energy secondary electrons with energies ranging from 0.1 to tens of electron-volts. Secondary electrons initiate destructive changes in DNA and RNA due to inelastic excitation and ionization processes [1], the consequences of which can be estimated by studying the most probable channels of fragmentation of these biomolecules. Among inelastic processes in electron-molecular collisions, the main ones are direct and dissociative ionization.

Monosaccharides (D-ribose, D-fructose, 2-deoxyribose, α-D-glucose) serve as an energy carrier and structural component for all living organisms. Therefore, changes in their molecular composition and the reactions that occur by interaction with electrons are extremely important for biology and radiation chemistry. Detailed studies of the fragmentation of various monosaccharides have been greatly facilitated by the development of mass spectrometric and spectroscopic tools [2-8]. Interest in monosaccharide fragmentation is also motivated by the potential role of secondary low-energy electrons in radiation damage to DNA [3, 4, 9], where the sugar fragment represents a major building block. The specificity of monosaccharide fragmentation is the loss of various amounts of H_2O molecules and the release of carbon-containing fragments consisting of CH_2O links [10].

[a]e-mail: gzavil@gmail.com (corresponding author), [b]demes.sandor@atomki.com, [c]remetoveyu@gmail.com

The mass spectrometric method of studying the processes of total and dissociative ionization is the most informative and allows, under identical experimental conditions, to obtain the complete mass spectrum of the molecule under study and to estimate the relative contribution of each dissociation fragment [10]. A detailed analysis of experimental and theoretical data for structural characterization of complex biomolecules is given in [11-14]. The most general direction of fragmentation of complex molecules during electron impact is simple breaking of hydrocarbon skeleton bonds to form oxonium-type ions, as well as dehydration of fragment ions. The presence of a hydroxyl group increases the probability of dissociative breakdown of molecules during electron impact ionization, and this usually leads to the absence of the parent molecular M^+ peak in the mass spectrum. This characteristic feature of electron ionization of polyatomic alcohols was previously found for molecules of glycerol, sorbitol, and ribose [15-18].

Theoretical and experimental studies of monosaccharide molecules were carried out in [13, 14, 17, 19-25]. In [19], the gas-phase structures of five five-carbon monosaccharides (D-ribose, D-lysose, 2-deoxy-D-ribose, D-xylose, and D-arabinose) were studied and it was shown that these monosaccharides are cyclic molecules. The use of density functional theory allowed us to determine the low-energy electronic structure of these molecules, which is pyranose. The multichannel computational method of Schwinger [20] found the constituents of DNA including nucleotide bases, phosphate esters and sugar-base models and found the shape resonances. In [21], experimental and theoretical results on photoionization of deoxyribose under synchrotron radiation are reported. Using high-level electronic structure methods, the authors calculated the adiabatic and vertical ionization energies of this molecule and analyzed the dynamics of dissociative photoionization of deoxyribose. In [22], using synchrotron radiation, the photofragmentation of deoxyribose at energies above the ionization threshold of this molecule was studied. The formation of a large number of molecular cation fragments with different intensities was observed. The study of biotin molecules, which has a similar structure to ribose, is devoted to [23]. It was shown that during dissociation the ring structure and the carboxyl group are broken, leading to the formation of fragment anions. In [12-14, 23-25] a detailed analysis of experimental and theoretical data on the structural characterization of complex biomolecules is given, and in the review [14] an analysis of the results on the study of the effect of low-energy electrons on biomolecules from the radiobiological point of view due to the formation of a transient anion is performed. A detailed study of the inelastic interaction of electrons with deoxyribose molecules was carried out in [24], in which the special role of secondary electrons in the irradiation of living cells was emphasized.

When molecules interact with electrons of low energies (0-10 eV), there is a process of electron capture by the molecule with the subsequent formation of negative ions. This process proceeds by resonance mechanisms and is well described in terms of energies and symmetry of vacant molecular orbitals (MOs) [26, 27]. The decay of negative ions is possible by either electron autodetaching or dissociation (fragmentation) and depends on some characteristics of the target molecule [26-29].

We systematically investigate the processes of single and dissociative ionization of biomolecules by electron impact and measure their thresholds by mass spectrometric method. It is in the region of ionization threshold energies that many aspects of atomic and molecular structure, which are determinant for energy dissipation in the interaction of electrons with multi-atomic molecules, are manifested.

2 Experimental setup

The apparatus and experimental methods have been described in detail earlier [17], so we will dwell only on the main parameters used in this experiment. A molecular beam (MB) from an effusive source was intersected at an angle of 90° with an electron beam of adjustable energy from 5 to 70 eV. The concentration of molecules in the zone of interaction with the electron beam was of the order of 10^{-11} cm^{-3}. The electron current could be varied within 0.05-0.5 mA, and the minimum electron energy spread was $\Delta E_{1/2}$ = 250 meV. The energy scale was calibrated to an accuracy no worse than ±0.08 eV. The ions formed as a result of the interaction were analyzed by the MX-7304A monopole mass spectrometer. In this experiment, for the ionization cross section measurements, the range of recorded masses and MB source temperature were: for *glucose* 10-170 Da, 425K, for *ribose* 10-150 Da, 375K.

In addition to mass spectra in the above mass range, a full cycle of measurements of energy dependences of fragment ion formation was performed. The most intense mass-fragments were determined from the mass spectra. Then these masses were set (not more than 20), the energy range was set, with a step of 0.25-1.0 eV, and simultaneous measurement of the energy dependences of fragment ion formation was carried out. The required measurement time was calculated by the formula

$$T_{\text{full}} = t_1 \cdot n \cdot C\,, \tag{1}$$

where t1 is the measurement time of one fragment, n is the number of fragments, C is the number of cycles which was determined depending on the value of the useful signal.

This technique allows us to determine the relative cross sections of dissociative ionization of initial molecules. To obtain the total relative ionization cross section, it is necessary to measure the total current of positive ions formed by the interaction between electrons and molecules.

At zero potentials at the deflecting electrodes of the mass spectrometer, the total current of positive ions formed as a result of interaction of the target molecules with electrons was measured at the collector. The energy was varied in steps of 0.2 eV in the near-threshold region of 5-20 eV and 1.0 eV in the range of 20-60 eV. In this mode, the energy dependences of the total relative ionization cross section (ionization functions) were measured, and the ionization potential of the molecules under study was determined by the least-squares method using the threshold regions of these dependences [17]. Registration and processing of the experimental results were carried out in automatic mode using special computer codes.

The experimental data were fitted to the curve given by the extended Wannier law convolved with the energy dispersion of the incident electron beam [17, 30]. The energy interval at which the fitting was performed was 6- 20 eV up to the inflection curve to the maximum. The determined ionization potential was stable with respect to the change of the energy interval. The background value was not more than 10%. The measurement error of the useful ionization signal was within 5-15%.

In experiments, two types of ionization cross sections (CSs) are measured: total ionization CSs [1, 31] and single ionization CSs (generally dissociative) of a certain fragment [32]. In the 1st case, all positive fragment ions of different masses formed in the collision of a molecule with an electron by various ionization processes, both without excitation and with excitation of the accompanying fragments: single, double, and dissociative ionization, are measured. Thus, in the experiments [1, 31], the total ionization CS of the amino acid molecules valine, glutamine, and glutamic acid was measured. In the 2nd case, only single-charged positive ions of a certain mass are measured [32]. Here, if the mass of a certain ion fragment is fixed, it is possible to directly measure the CS of the dissociative single ionization process in a direct

experiment and determine the energy appearance of this fragment. If it is the mass of the ion of the parent molecule, the CS and threshold of its single ionization process will be measured.

3 Results and discussion

3.1 Glucose and ribose formulas

By their chemical nature, monosaccharides are aldehyde or keto alcohols [18], they are divided into two groups: D- and L- forms. The most important representatives of aldopentoses are D-ribose, D-deoxyribose and aldohexoses are D-glucose. One of the fundamental properties of monosaccharides is due to the manifestation of different types of isomerism. Isomers, have the same molecular formula but differ in the arrangement of atoms in space. Glucose ($C_6H_{12}O_6$) is one of the most common monosaccharides of hexose group, the most important source of energy in living cells, it is a part of various oligosaccharides, polysaccharides and some glycoproteins. Ribose ($C_5H_{10}O_5$) - belongs to the group of aldopentoses, and in furanose form D-ribose is a part of RNA.

Glucose has four asymmetric carbon atoms - chiral centers, each of which is bound by substituent - hydrogen atom and OH. This structural formula suggests the possibility of 16 stereoisomers, among which 8 pairs are enantiomers. One of these 8 pairs consists of D- and L- optical isomers, their structural features and relations between atoms are displayed using E. Fischer's projection formulas: the number of vertical and horizontal lines corresponds to the number of asymmetric carbon atoms, the aldehyde group is written above the vertical line, and the H and OH atoms are written at the ends of the horizontal lines. The linear formulas of E. Fisher (**a** in Fig. 1) make it possible to visually explain most of the physical and chemical properties of monosaccharides.

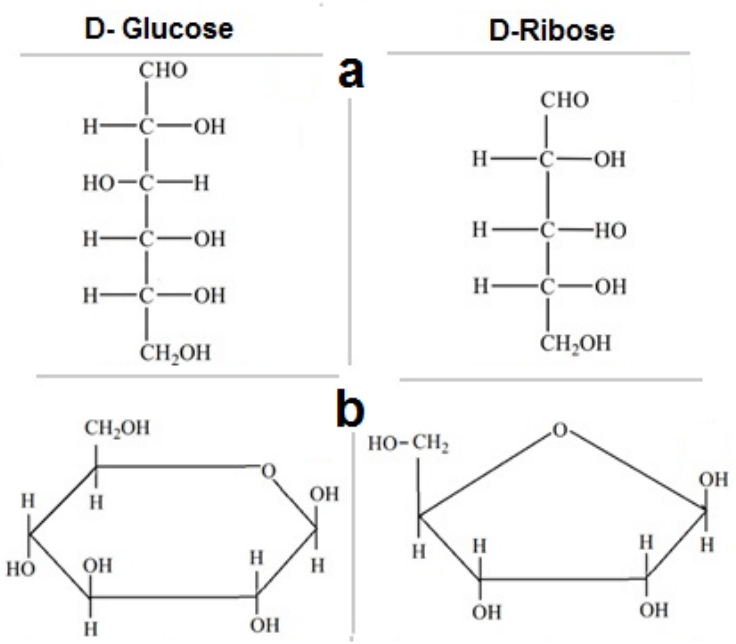

Figure 1 Linear (**a**) and cyclic (**b**) glucose and ribose forms

Some properties are not shown by these formulas because not all hydroxyl groups have the same features. Therefore, to explain these properties, structural formulas are presented in cyclic form (**b** in Fig. 1). Ring forms are spatial isomers that can have five-membered (furanose) and six-membered (pyranose) rings. The cyclic form of glucose is a five-membered ring in which the fifth and fourth carbon atoms are as close as possible to the first, which ensures that the carbonyl group of the hydrogen atom from the hydroxyl is attached to the oxygen. D-ribose has two cyclic forms as β-D-ribofuranose and β-D-ribose (deoxyribose). D-ribose belongs to the group of polyhydric hydrocarbon alcohols (polyols).

3.2 Calculations for single ionization cross sections of monosaccharide molecules by electron impact

To estimate the summarized single ionization cross sections of molecules $\sigma(E)=\sum_k \sigma_k(E)$ for the k-th MOs taken into account, the following pair collision models are used: the dipole Binary-Encounter-Dipole (BED), the semiclassical Binary-Encounter-Bethe (BEB) [25, 33, 34], and the classical Gryzinski approximation (Gryz) [35] (also see [36]). We calculate CS in the BEB and Gryz models.

In the BEB model, the expression for a single ionization CS of a molecule (electron removal) from the k-th MO is as follows:

$$\sigma_k(t_k)=\frac{S_k}{t_k+u_k+1}\cdot\left\{\frac{1}{2}Q_k\cdot\left(1-\frac{1}{t_k^2}\right)\cdot\ln t_k+(2-Q_k)\cdot\left[\left(1-\frac{1}{t_k}\right)-\frac{\ln t_k}{t_k+1}\right]\right\} . \qquad (2)$$

Here $t_k=E/B_k$, E – is the kinetic energy of the incoming electron, B_k – is the binding energy of the electron removed from the k-th MO, $u_k=U_k/B_k$, where U_k – is the average kinetic energy of electrons at the k-th MO. The values S_k, Q_k are found from the expressions:

$$S_k=4\pi\cdot a_0^2\cdot N_k\cdot(R/B_k)^2 \;;\; Q_k=\frac{2\cdot B_k\cdot M_k^2}{N_k\cdot R} \;;\; M_k^2=\frac{R}{B_k}\cdot\int_0^\infty\frac{1}{w_k+1}\cdot\frac{\mathrm{d}f(w_k)}{\mathrm{d}w_k}\mathrm{d}w_k \;, \qquad (3)$$

Where $w_k=W/B_k$, W – is the kinetic energy of the removed electron, $\mathrm{d}f(w_k)/\mathrm{d}w_k$ – is the differential oscillator strength for the molecule, N_k – is the number of electrons on the k-th MO, R = 13.6058 eV is the Rydberg constant, $a_0=5.2918\cdot10^{-11}\,m$ is the Bohr radius (atomic unit of length). The value of Q_k is assumed to be equal to 1 [25].

The expression for the single ionization CS of a molecule from the k-th MO in the Gryzinski approximation is as follows:

$$\sigma_k(t_k)=\frac{\sigma_0}{B_k^2}\cdot\frac{1}{t_k}\cdot\left(\frac{t_k-1}{t_k+1}\right)^{3/2}\cdot\left\{1+\frac{2}{3}\cdot\left(1-\frac{1}{2t_k}\right)\cdot\ln\left[2.7+(t_k-1)^{1/2}\right]\right\} \;, \qquad (4)$$

where σ_0 = 6.56 × 10^{-18} eV^2 m^2. The CS in this approximation is determined only by the binding energy B_k of the electron on the MO.

Using two methods, Hartree-Fock (HF) and density functional theory (DFT), the structure of D- and L-forms of glucose molecules were calculated using the Gaussian 16 code [37]. The energy characteristics of their MOs – binding B_k and average kinetic U_k energies – were used to calculate the summarized single ionization CSs based on the MOs (48 for Glc and 40 for Ribf).

The ionization potentials of glucose and ribose molecules calculated from binding energies B_{48}^{HOMO} and B_{40}^{HOMO} (I = -B^{HOMO}) and the measured experimental values are presented in Table 1. We see that the HF data are about 4 eV larger than the data obtained by the DFT method.

Table 1. Ionization potentials (in eV) of glucose and ribose molecules

Method	D-Glucose (Glc)	D-Ribose (Ribf)
Experiment	12.25±0.25	10.46±0.25
Theoretical calculations		
HF D-form	11.56	11.15
HF L-form	11.63	11.41
DFT D-form	7.64	7.31
DFT L-form	7.71	7.60

It is the appearance of fragment ions as a result of the dissociative ionization process that determines the partial ionization and the total ionization CSs and possible changes in the structure of their energy dependencies – small maxima, breaks, irregularities. In the case of glucose molecule the most intense peaks in the mass spectra correspond to fragment ions: CHO^+, CH_3O^+, $C_2H_3O^+$, $C_2H_4O_2^+$, $C_2H_5O_2^+$, $C_3H_5O_2^+$, $C_3H_7O_3^+$, which form a series of peaks with a mass difference of 1 Da [30]. As can be seen, in addition to CH_3O^+, they contain from 2 to 4 carbon atoms, as well as the aldehyde group CHO^+. In the case of the D-ribose molecule a general characteristic of the mass spectra is the presence of groups of lines, the central ones being the peaks corresponding to ions with m/z = 29, 43, 60, 73, 86 and products of secondary fragmentation of fragmentation ions - CO^+ and CH_3^+ [17].

At low energies, close to the threshold, the total ionization CS is determined as a rule by the single ionization CS of the parent molecules. This is valid for the glucose molecule. But in the case of ribose molecule, the appearance energy of $C_4H_9O^+$ cation is 10.84 eV [17], which is close to the ionization energy of the molecule 10.46 ± 0.25 eV. Therefore, in the near-threshold region, the total ionization cross section is determined by the partial ionization cross sections of the molecule and dissociative ionization of the $C_4H_9O^+$ cation formation (see also [26-29, 38, 39]).

3.3 Calculations of the cross sections of single ionization of glucose and ribose molecules by electron impact and the absolute values of the experimental total ionization cross sections

One of the simplest ways to obtain absolute values of the measured CSs is to normalize their relative counts to sufficiently reliable theoretical data. In the experiments presented in this paper, we used the theoretical single ionization CSs to normalize the experimental total ionization CSs in the pre-threshold region. Since we did not take into account the dissociative ionization process leading to the appearance of the $C_4H_9O^+$ fragment ion and did not calculate the corresponding cross section, our normalization of the relative experimental values to the theoretical cross section of one-electron ionization gives an underestimated value of the total ionization cross section of the ribose molecule. To calculate the single ionization CSs, we use the (2)-(4) formulas of the two pair collision models.

Glucose. The measured threshold of single ionization of the glucose molecule is 12.25 ± 0.25 eV (see Table 1). Fig. 2 presents a comparison of the measured normalized (absolute values) total CSs and theoretical summarized CSs for the D- and L-forms of the glucose molecule. We see that the Gryz-DFT energy behavior CS is similar to the measured one. In general, the CSs with DFT MOs increase faster than

those with MOs calculated in the HF approximation. Also, Gryz CSs increase faster than BEB CSs. The absolute values of the measured total CSs of ionization of the glucose molecule are given in Table 2.

The normalization of the relative experimental CSs values at 11 eV was performed on the Gryz-DFT single ionization CS for the D-form. In this case, the Gryz-DFT CS (curve 2) was shifted toward higher energies by 1 eV. As mentioned above, the energy characteristics of the MO of both forms of the glucose molecule are very similar (see Table 1). Therefore, it is expected that the single ionization CSs will be similar in magnitude. For the L-form, the same absolute values are plotted in Fig. 2, where the Gryz-DFT CS (curve 2) is also shifted by 1 eV to the right. We can see that the experimental total ionization CS exceeds the summarized theoretical single ionization CSs, increases faster with increasing collision energy, and the maximum value is 84.31×10^{-20} m^2 at 40.6 eV.

Ribose. The measured threshold of single ionization of the ribose molecule is 10.46 ± 0.25 eV (see Table 1). Fig. 3 presents a comparison of the normalized total ionization CSs measured up to 69.59 eV and the summarized theoretical CSs for the D- and L-forms of the ribose molecule. We can see that the energy behavior of the Gryz-DFT CS is similar to the measured one. In general, the CSs with DFT MOs increase faster than those with MOs calculated in the HF approximation. Also, Gryz cross-sections increase faster than BEB CSs. The absolute values of the measured total ionization CSs of the ribose molecule are given in Table 3.

The normalization of the relative experimental values at 12.65 eV was performed on the Gryz-DFT single ionization CS for the D-form. In this case, the Gryz-DFT CS (curve 2) was shifted toward higher energies by 3.15 eV, which is the difference between the experimental ionization threshold and the binding energy of the HOMO orbital. The background was subtracted from the experimental values, the average energy dependence of which is a straight line $y=0.22327+0.01375\cdot E$. As mentioned above, the energy characteristics of the MOs of both forms of the ribose molecule are very close. Therefore, it is expected that the single ionization CSs will be similar in size. For the L-form in Fig. 3, the same absolute values are plotted, where the Gryz-DFT cross section (curve 2) is also shifted by 3.15 eV to the right. We can see that the experimental total ionization CS exceeds the summarized theoretical single ionization CSs, increases faster with increasing collision energy, and the maximum value is 65.63×10^{-20} m^2 at 43.1 eV.

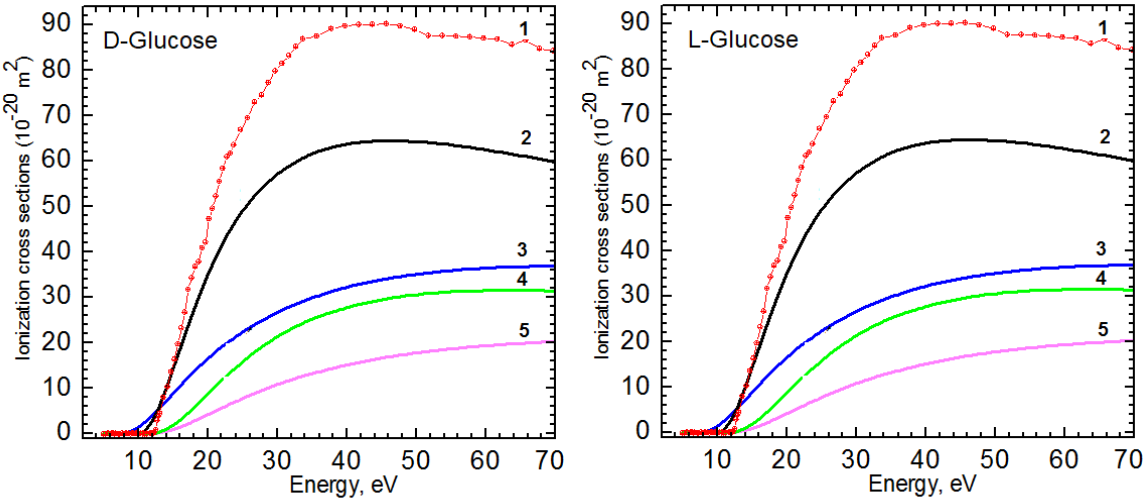

Figure 2 Ionization cross sections of the D- and L-forms of the glucose molecule. The experimental total ionization cross section are normalized to the Gryz-DFT calculation at 11 eV (D-form) – 1 (ooo). Calculations of the summarized cross sections of single ionization: 2 – Gryz-DFT; 3 – BEB-DFT; 4 – Gryz-HF; 5 – BEB-HF.

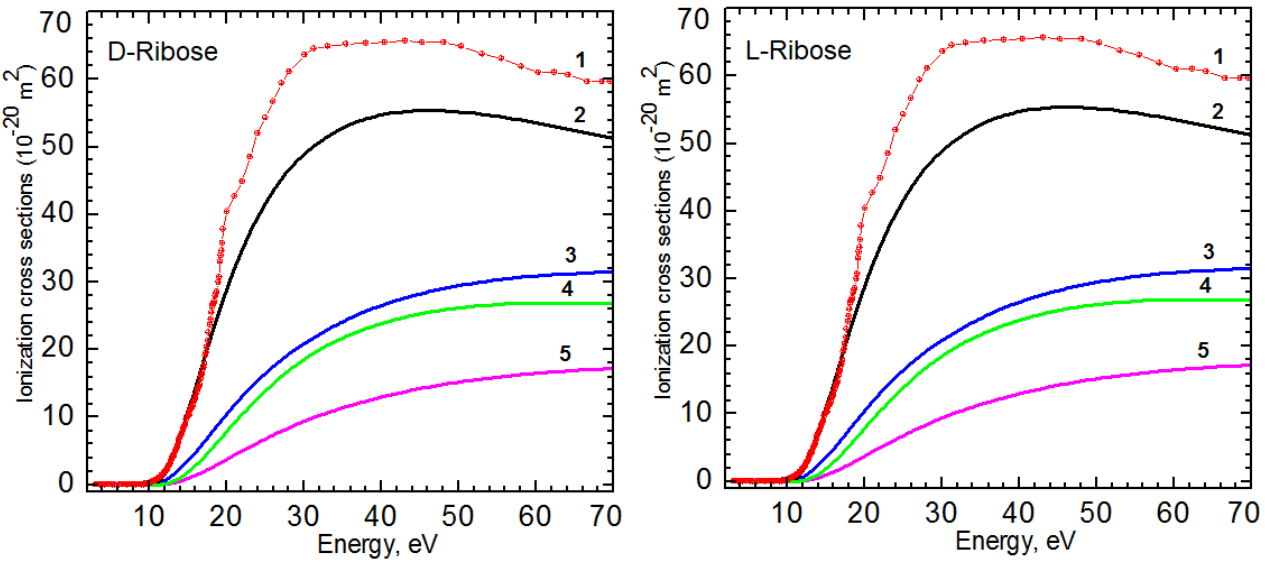

Figure 3 Ionization cross sections of the D- and L-forms of the ribose molecule. The experimental total ionization cross section are normalized to the Gryz-DFT calculation at 12.65 eV (D-form) – 1 (ooo). Calculations of the summarized cross sections of single ionization: 2 – Gryz-DFT; 3 – BEB-DFT; 4 – Gryz-HF; 5 – BEB-HF.

Table 2. Absolute values of the experimental total ionization cross-section of glucose molecule by electron impact.

E, eV	CS, 10^{-20} m^2	*E*, eV	CS, 10^{-20} m^2	*E*, eV	CS, 10^{-20} m^2
9.99	0.17	18.59	46.45	39.59	84.31
10.19	0.25	19.09	49.02	41.59	84.31
10.39	0.81	19.59	51.98	43.59	84.40
10.59	2.81	20.09	54.63	45.59	84.03
10.79	3.70	20.59	57.04	47.59	83.39
10.99	4.34	21.09	57.84	49.59	82.12
11.49	7.55	21.59	59.44	51.59	82.03
12.09	9.71	22.59	62.65	53.59	81.88
12.59	12.76	23.59	65.06	55.59	81.76
13.09	15.39	24.59	68.27	57.59	81.53
13.59	18.54	25.59	69.71	59.59	81.40
14.09	21.74	26.59	72.28	61.59	80.27
14.59	25.11	27.59	74.68	63.59	81.08
15.09	29.69	28.59	76.29	65.59	79.39
15.59	32.17	29.59	77.89	67.59	78.99
16.09	34.50	30.59	79.78	69.59	78.83
16.59	35.46	31.59	81.30	71.59	78.51
17.09	38.35	33.59	81.94	73.46	78.52
17.59	39.39	35.59	83.51	–	–
18.09	44.20	37.59	84.00	–	–

3.4 Calculation of the ionization cross sections of the highest (HOMO) molecular orbitals by electron impact

It is important to determine the contribution in the single ionization CS from the highest occupied (HOMO) orbital into the summarized CS. This relative contribution from the higher MO is defined by the expression:

$$P(E)=[\sigma_{k_{HOMO}}(E)/\sum_{k=k_{HOMO}}^{k=(k_{HOMO}-n+1)}\sigma_k(E)]\cdot 100\%\ ,$$

here k is the number of MO, n is the number of MO taken into account at a given collision energy E. It is obvious that the contribution from HOMOs is dominant at initial energies. The magnitude of the contribution $P(E)$ and the number of molecular orbitals n in the total cross section depend on the collision energy.

Glucose. Fig. 4 shows the energy dependence of the relative contribution of $P(E)$ from the highest MO ($k_{\mathrm{HOMO}} = 48$) to the calculated summarized Gryz-DFT $\sigma(E)$ single ionization CS of the D-form of the glucose molecule. This contribution is compared with the behavior of the single ionization CSs of the summarized $\sigma(E)$ and higher MO $\sigma_{k_{HOMO}}(E)$. The latter CS, $\sigma_{k_{HOMO}}(E)$, reaches a maximum of 4.442×10^{-20} m^2 at 29 eV. The contribution of $P(E)$ decreases rapidly with increasing collision energy: in the interval from the threshold of 8 eV to 20 eV, it decreases by a factor of more than 9, from 94.2 to 10.5%. In Fig. 4 we can see that at energies close to the ionization threshold, the contribution of $P = 100\%$, i.e. the summarized CS is determined by one high-lying MO ($n = 1$). Starting from 30 eV, the summarized CS is determined by all 36 (from 13 to 48) MOs (n=36). In general, the contribution $P(E)$ of the HOMO orbital is quite significant: 13.9% at 15, 8.2% at 30, 6.8% at 50, and ~ 6.2% at 70 eV.

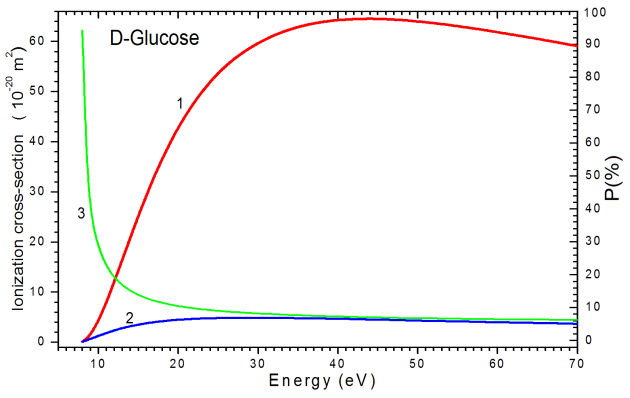

Figure 4 Energy dependence of the calculated Gryz-DFT cross-sections of single ionization of the D-form of the glucose molecule (in 10^{-20} m^2) and the relative contribution from the higher $k_{\mathrm{HOMO}} = 48$ MO. 1 – $\sigma(E)$, 2 – HOMO $\sigma_{k_{HOMO}}(E)$, 3 – relative contribution $P(E)$

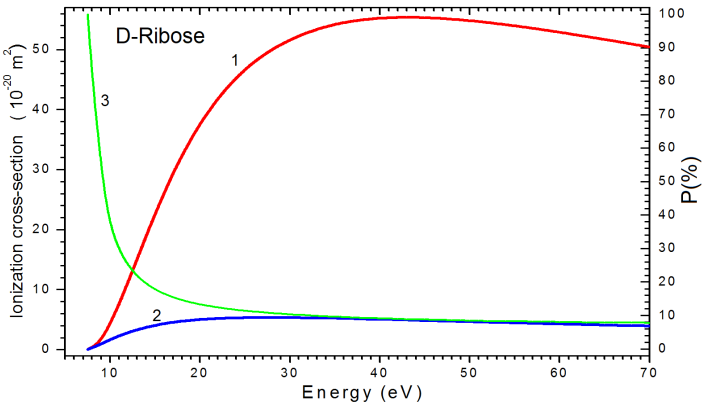

Figure 5 Energy dependence of the calculated Gryz-DFT cross-sections of single ionization of the D-form of the ribose molecule (in 10^{-20} m^2) and the relative contribution from the higher $k_{\mathrm{HOMO}} = 40$ MO. 1 –summarized σ(E), 2 – HOMO $\sigma_{k_{HOMO}}(E)$, 3 – relative contribution $P(E)$

Table 3. Absolute values of the experimental total ionization cross-section of ribose molecule by electron impact.

E, eV	CS, 10^{-20} m^2	E, eV	CS, 10^{-20} m^2	E, eV	CS, 10^{-20} m^2	E, eV	CS, 10^{-20} m^2
10.39	0.43	13.49	5.26	16.60	14.82	20.07	40.38
10.49	0.48	13.61	5.54	16.71	15.66	21.07	42.70
10.60	0.58	13.70	5.81	16.83	16.16	22.07	44.80
10.71	0.60	13.81	6.25	16.93	16.60	23.07	48.53
10.84	0.65	13.94	6.68	17.05	17.30	24.07	52.02
10.94	0.74	14.02	6.96	17.17	17.91	25.07	54.35
11.03	0.80	14.15	7.19	17.26	19.14	26.07	56.68
11.18	0.87	14.25	7.54	17.39	19.61	27.07	59.41
11.21	0.95	14.38	8.07	17.52	20.41	28.07	61.08
11.34	1.02	14.50	8.41	17.62	21.34	30.07	63.61
11.49	1.20	14.60	8.71	17.67	22.53	31.27	64.51
11.59	1.347	14.73	8.93	17.85	23.72	33.07	64.83
11.69	1.50	14.83	9.65	17.95	24.51	35.47	65.17
11.84	1.56	14.94	9.99	18.06	25.46	38.07	65.29
11.91	1.73	15.06	10.32	18.20	26.45	40.37	65.46
12.05	1.91	15.17	10.29	18.29	26.75	43.07	65.63
12.17	2.08	15.29	10.91	18.39	26.76	45.27	65.40
12.29	2.20	15.39	11.32	18.48	27.07	48.07	65.41
12.41	2.49	15.47	11.56	18.59	27.94	50.37	64.89
12.48	2.71	15.63	11.44	18.71	28.26	53.07	63.77
12.59	2.87	15.72	11.76	18.82	28.59	55.47	63.04
12.70	3.02	15.81	12.36	18.94	29.93	58.07	61.92
12.87	3.30	15.92	12.59	19.06	30.70	60.31	61.04
12.91	3.68	16.03	12.80	19.16	32.98	62.33	61.01
13.07	3.96	16.14	13.46	19.29	33.95	64.18	60.67
13.18	4.21	16.28	13.91	19.39	34.66	66.59	59.69
13.24	4.42	16.41	14.22	19.49	35.72	68.47	59.66
13.38	4.95	16.50	14.45	19.61	37.85	69.59	59.62

Ribose. Fig. 5 shows the energy dependence of the relative contribution of $P(E)$ from the highest MO, k_{HOMO}=40 to the calculated summarized Gryz-DFTCS $\sigma(E)$ of the single ionization of the D-form of the ribose molecule. This contribution is compared to the behavior of the single ionization CSs of the summarized $\sigma(E)$ and higher MO $\sigma_{k_{HOMO}}(E)$. The latter cross section, $\sigma_{k_{HOMO}}(E)$, reaches a maximum of 5.337 × 10^{-20} m^2 at 27.5 eV. The contribution of $P(E)$ decreases rapidly with increasing collision energy: in the interval from the threshold of 7.5 eV to 20 eV, it decreases by a factor of more than 7, from 100 to 13/3%. Fig. 5 shows that at 7.5 eV, i.e. at the ionization threshold, the contribution of P = 100%, i.e., the summarized CS is determined by one higher MO (n = 1), while at 8 eV P = 82.6%. Starting from 30 eV, the summarized CS is determined by all 30 (from 11 to 40) MOs (n = 30). In general, the contribution of the $P(E)$ HOMO orbital is quite significant: 17.9% at 15, 10.3% at 30, 8.5% at 50, and ~ 7.8% at 70 eV.

Note, that the contributions of the HOMO-1, HOMO-2 to the Gryz-DFT $\sigma(E)$ also rapidly decrease from the threshold B_k and at finite energies their values are: at 73.7 eV (Glc) – 5.8 and 5.7% and at 68.5 eV (Ribf) – 7.2 and 6.4%.

3.5 Summarized cross-sections of single ionization of atomic and molecular fragments of glucose and ribose molecules in the BEB model

Glucose ($C_6H_{12}O_6$) and ribose ($C_5H_{10}O_5$) molecules, as organic molecules, consist of a corresponding number of C, H, O atoms and a certain number of fragments (see their linear forms above). It is worth to compare the summarized single ionization CSs of a molecule and the corresponding single ionization CSs of all its atoms and all its fragments.

In the case of the D-form of glucose and ribose molecules, the summarized single ionization CSs of the atoms σ_{at}(Glc), σ_{at}(Ribf) and fragments σ_{frag}(Glc), σ_{frag}(Ribf) are as follows:

$$\sigma_{at}(\text{Glc}) = 6\sigma(\text{C}) + 12\sigma(\text{H}) + 6\sigma(\text{O}) , \quad (5)$$

$$\sigma_{frag}(\text{Glc}) = 4\sigma(\text{CH}) + \sigma(\text{CH}_2) + 5\sigma(\text{OH}) + \sigma\sigma(\text{COH}) , \quad (6)$$

$$\sigma_{at}(\text{Ribf}) = 5\sigma(\text{C}) + 10\sigma(\text{H}) + 5\sigma(\text{O}) , \quad (7)$$

$$\sigma_{frag}(\text{Ribf}) = 3\sigma(\text{CH}) + \sigma(\text{CH}_2) + 4\sigma(\text{OH}) + \sigma(\text{COH}) . \quad (8)$$

In such a comparison, it is necessary that all CSs are calculated in the same approximation. We choose the BEB model because it is already well-tested. Of course, there are many ways to separate fragments in complex molecules. But, in our opinion, this will not significantly change the summarized ionization CS σ_{frag}. To a greater extent, the value and behavior of this CS depends on the approximation in which it is calculated (BEB or Gryz) and to a lesser extent on the method of calculating the fragment MO (DFT or HF) (see Figs. 2 and 3).

The basis for this representation of the ionization CSs by expressions (5)-(8) is the model of independent atoms as it was used in the problem of electron scattering by molecules. The imaginary part of the optical potential describing the interaction of the incoming electron with the molecule determines the inelastic CS, which is the sum of all inelastic CSs.

The ionization potentials of atoms are as follows (in eV) [40]: I(H) = 13.5985; I(S) = 11.260; I(O) = 13.618. The ionization potentials of molecular fragments and the binding energy of electrons on HOMO are as follows (in eV): I(CH) = 10.9 [41], B_{HOMO} = 10.64 [40]; $I(CH_2)$ = 10.396 [41], B_{HOMO} = 10.40 [40]; I(OH) = 13.18 [41], I(OH) = 13. 0170 ± 0.0002 [42]; I(SO) = 14.0142 ± 0.0003 [43], B_{HOMO} = 14.01 [40]; I(SO) = 8.14 ± 0.14 [44], B_{HOMO} = 9.20 [40]. At a given energy of the ionizing electron, the contribution to the process is given by those fragments whose ionization threshold is less than this electron energy. According to the BEB formula, the contribution to the ionization CS is given by those MOs whose binding energy, starting from B_{HOMO}, is less than the electron energy.

In the literature, the BEB approach has been used to calculate the single ionization CSs of the above mentioned atoms H [45], C and O [46], and fragments CH [47], CH_2 and CO [48], OH [49], COH [50]. Note that the calculated CSs are in good agreement with the experimental data (see [51-54] in [51]). At their maxima, they are within the measurement errors. In [46], two approximations, BEB and BED, were used for the ionization of a hydrogen atom (see expressions (3)-(4) above). In this case, the BEB approximation gives better agreement with the experiment [55].

Glucose. In Fig. 6, we compare the BEB CSs of the single ionization of atoms 12σ(H), 6σ(C), 6σ(O),the summarized atomic $\sigma_{at}(E)$ (see (5)) and the summarized BEB-DFT $\sigma(E)$ CSs of the glucose molecule. In Fig. 7, we compare the single ionization CSs of fragments 4σ(CH), $\sigma(CH_2)$, 5σ(OH), σ(COH),

the summarized of $\sigma_{frag}(E)$ (see (6)) and the BEB-DFT $\sigma(E)$ CSs of the glucose molecule. From Figs. 6 and 7, we can see that the total cross section of the single ionization of atoms $\sigma_{at}(E)$ is slightly higher than the summarized CS of the fragment ionization $\sigma_{frag}(E)$. The main contribution to the $\sigma_{at}(E)$ CS is made by the ionization of six carbon and twelve hydrogen atoms (up to 95 eV), and to the $\sigma_{frag}(E)$ CS by the ionization of four CH and five OH fragments. The CSs $\sigma_{at}(E)$ and $\sigma_{frag}(E)$ are much smaller than the summarized BEB-DFT $\sigma(E)$ CS of a single ionization of a glucose molecule. The energy behavior of the CSs is similar due to the fact that the BEB approximation formulas were used.

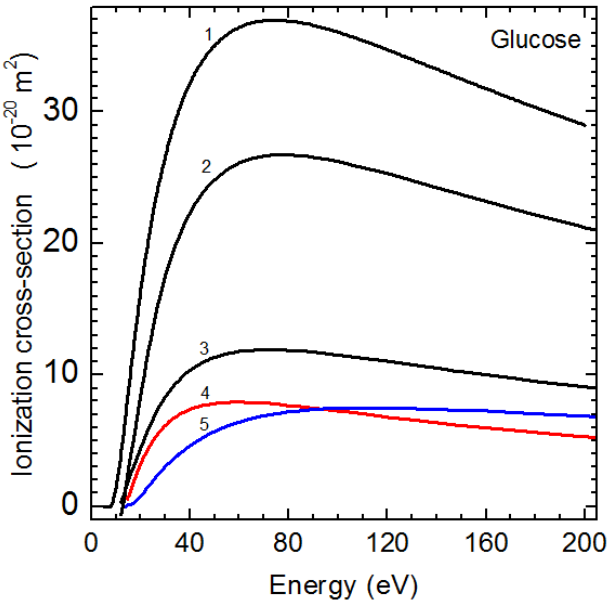

Figure 6 Ionization cross sections of glucose molecule atoms. The calculated cross sections of single ionization: BEB-DFT for the glucose molecule $\sigma(E)$ – 1, summarized for all atoms $\sigma_{at}(E)$ – 2 and individual atoms 6σ(C) – 3, 12σ(H) – 4, 6σ(O) – 5

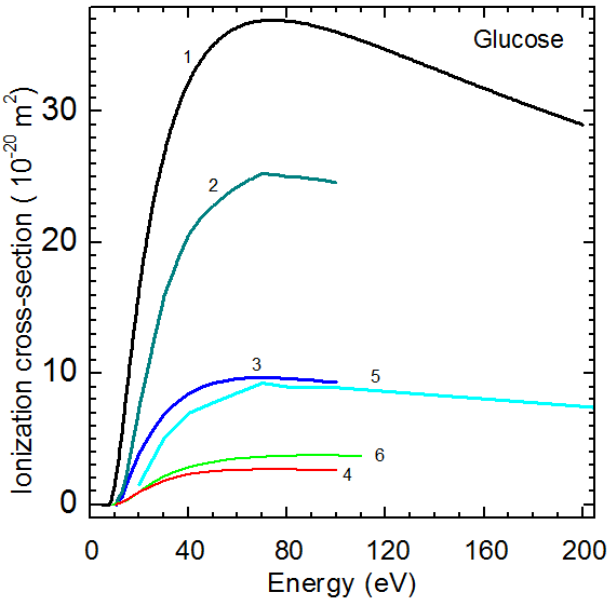

Figure 7 Ionization cross sections of structural fragments of a glucose molecule. The calculated cross sections of single ionization: BEB-DFT for the glucose molecule $\sigma(E)$ – 1, summarized for all fragments $\sigma_{frag}(E)$ – 2 and individual fragments σ(CH) – 3, $\sigma(CH_2)$ – 4, 5σ(OH) – 5, σ(COH) – 6.

Ribose. In Fig. 8, we compare the BEB CSs of the single ionization of atoms 10σ(H), 5σ(C), 5σ(O), the total atomic cross section $\sigma_{at}(E)$ (see (7)), and the summarized BEB-DFT $\sigma(E)$ of the ribose molecule. In Fig. 9, we compare the single ionization CSs of fragments 3σ(CH), $\sigma(CH_2)$, 4σ(OH), σ(COH), the summarized CSs of $\sigma_{frag}(E)$ (see (8)) and the BEB-DFT $\sigma(E)$ of the ribose molecule. From Figs. 8 and 9, we can see that the summarized CS of the single ionization of atoms $\sigma_{at}(E)$ is almost equal to the summarized CS $\sigma_{frag}(E)$ of fragment ionization. The main contribution to the $\sigma_{at}(E)$ CS is made by the ionization of five carbon and ten hydrogen atoms (up to 90 eV), and to the $\sigma_{frag}(E)$ CS by the ionization of three CH fragments and four OH fragments. The CSs $\sigma_{at}(E)$ and $\sigma_{frag}(E)$ are smaller than the summarized BEB-DFT $\sigma(E)$ CS of a single ionization of a glucose molecule. The energy behavior of the CSs is also similar.

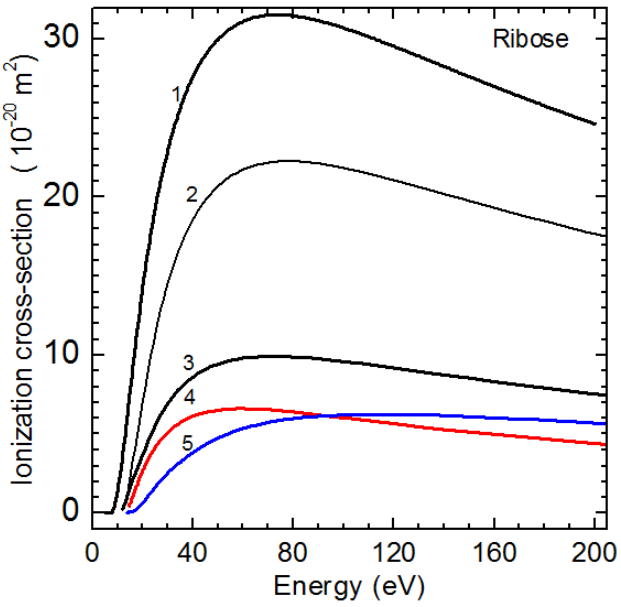

Figure 8 Ionization cross sections of ribose molecule atoms. The calculated cross sections of single ionization: BEB-DFT for the ribose molecule $\sigma(E)$ – 1, summarized for all atoms $\sigma_{at}(E)$– 2 and individual atoms 5σ(C) – 3, 10σ(H) – 4, 5σ(O) – 5

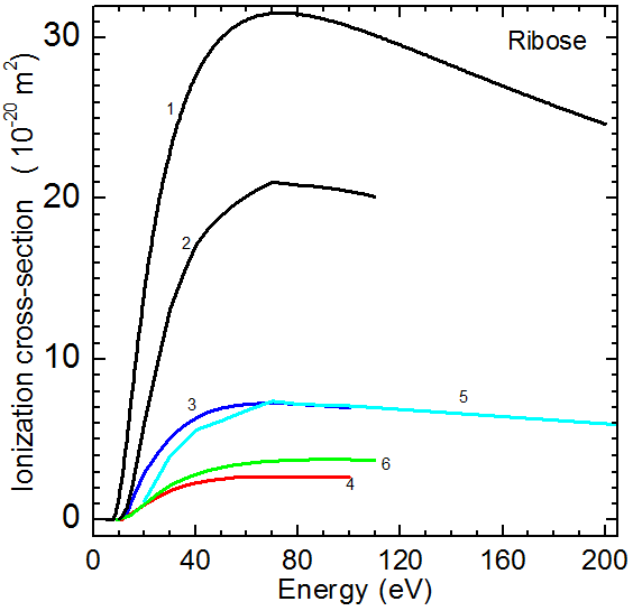

Figure 9 Ionization cross sections of structural fragments of a ribose molecule. The calculated cross sections of single ionization: BEB-DFT for the ribose molecule $\sigma(E)$ – 1, summarized for all fragments$\sigma_{frag}(E)$ – 2 and individual fragments 3σ(CH) – 3, $\sigma(CH_2)$ – 4, 4σ(OH) – 5, σ(COH) – 6

4 Conclusions

The total relative ionization cross sections of glucose and ribose molecules have been measured in the energy range of 5-70 eV by mass spectrometry. By approximating the threshold region of the energy dependence of the cross sections, the ionization potentials of the studied molecules have been determined. Using standard packages of quantum-chemical software, the structure of two forms (D, L) of glucose and ribose molecules was calculated *ab initio* by Hartree-Fock and density functional theory methods. The ionization potentials of these molecules have been estimated in the molecular orbitals approximation. Their values obtained by the density functional theory method are smaller than the measured ones, while those obtained by the Hartree-Fock method are close to them.

The summarized cross sections of single ionization of D- and L-forms of glucose and ribose molecules by electron impact calculated by the Binary-Encounter-Bethe and Gryzinsky models have been compared with the energy characteristics of molecular orbitals calculated by the above mentioned methods. The cross sections calculated by the Gryzinsky model with the characteristics of molecular orbitals found by density functional theory were used to normalize the measured total cross sections at energies close to threshold. This allowed us to obtain absolute values of the measured ionization cross sections. The relative contribution of the HOMO orbital to the summarized ionization cross section at an electron energy of 70 eV is: ~6% for glucose molecule and ~8% for ribose. The Binary-Encounter-Bethe calculated ionization cross sections of glucose and ribose molecules exceed the summarized ionization cross sections of atoms and structural fragments of these molecules.

Author contributions

A. Zavilopulo contributed to experiments and analysis of their results, S. Demes, and E. Remeta contributed to calculations and analysis of the theoretical results. All authors participated in the discussion of the results and in the preparation of the manuscript. S Demes (https://orcid.org/0000-0002-2783-7172), A. Zavilopulo (https://orcid.org/0000-0001-8334-2804) and E. Remeta (https://orcid.org/0000-0001-9799-7895)

Data Availability Statement

This manuscript has associated data in a data repository on the web-site of the Institute of Electron Physics (http://iep.org.ua/).

References

1. A.N. Zavilopulo, A.I. Bulhakova, S.S. Demes, E.Yu. Remeta, A.V. Vasiliev, Eur. Phys. J. D 75:287 (2021). doi.org/10.1140/epjd/s10053-021-00294-2
2. G.W. Cline, G.I. Shulman, J. Biological Chemistry **270**, No. 47, 28062 (1995)
3. U. Hannestad, A. Lundblad, Clinical Chemistry **43**, No. 5, 794 (1997)
4. P. Papp, P. Shchukin, J. Kočíšek, Š. Matejčík, J. Chem. Phys. **137**, 105101 (2012) http://dx.doi.org/10.1063/1.4749244
5. P. Sulzer, S.Ptasin'ska, F. Zappa, B.Mielewska, A.R. Milosavljevic, P. Scheier, T.D. Märk, J. Chem. Phys. **125**, 044304 (2006) DOI:10.1063/1.2222370
6. H.D. Flosadottir, I. Bald, J. Mass Spectrom. **305**, 50 (2011)
7. V.F. Taylor, R.E. March, H.P. Longerich, C.J. Stadey, J. Mass Spectrom. **243**, 71 (2005)
8. A. Frolov, P. Hoffmann, R. Hoffmann, J. Mass Spectrom. **41**(11), 1459 (2006) DOI: 10.1002/jms.117
9. H.W. Jochims, M. Schwell, J.L. Chotin et al, Chem. Phys. **298**, 1-3. 279 (2004)
10. J. Beynon, *Mass spectrometry and its applications in organic chemistry* (Mir, Moscow, Mir, 1964)
11. W.A. Szarek, S.-L. Korppi-Tommola, O.R. Martin, V.H. Smith Jr., Canadian Journal of Chemistry **62**(8), 1506 (1984) https://doi.org/10.1139/v84-257
12. Yang Gao, Jiexun Bu, Zhou Peng, Biwei Yang. Journal of Spectroscopy 2014 (2014), Article ID 570863, 10 pages
13. I. Baccarelli, I. Bald, F.A. Gianturco, E. Illenberger, J. Kopyra, Phys. Rep. **508** 1 (2011) http://dx.doi.org/10. 1016/j.physrep.2011.06.004
14. L. Sanche, Eur. Phys. J. D **35,** 367 (2005) http://dx.doi.org/10.1140/epjd/e2005-00206-6
15. A.N. Zavilopulo, O.B. Shpenik, P.P. Markush, E.E. Kontrosh, Tech. Phys. **40**, 829 (2014)
16. I. Chernyshova, P. Markush, A. Zavilopulo, O. Shpenik, Eur. Phys. J. D **69**, 80 (2015) http://dx.doi.org/10.1140/epjd/e2015-50641-7
17. A.N. Zavilopulo, O.B. Shpenik, A.N. Mylymko, V.Yu. Shpenik, Int. J. Mass Spectr. **441**, 1 (2019) https://doi.org/10.1016/j.ijms.2019.03.008
18. L.P. Guler, Ying-Qing Yu, H.I. Kenttama, J. Phys. Chem. A **106**, 6754 (2002)
19. C. Winstead, V. McKoy, Journal of Physics: Conf. Ser. **388**, 012017 (2012) doi: 10.1088/1742-6596/388/012017
20. D. Ghosh, A. Golan, L.K. Takahashi, A.I. Krylov, M. Ahmed, J. Phys. Chem. Lett. **3**, 97 (2012) dx.doi.org/10.1021/jz201446r
21. G. Vall-llosera, K. Jakubowska, M. Stankiewicz, M.A. Huels, M. Coreno, A. Kivimki, E. Rachlew, Chem. Phys. Chem **9**, 1020 (2008) DOI: 10.1002/cphc.200700635
22. A. Keller, J. Kopyra, K.V. Gothelf, I. Bald, New Journal of Physics **15** 083045 (2013) doi: 1367-2630/13/083045

23. I. Baccarelli, F.A. Gianturco, E. Scifoni, A.V. Solov'yov, E. Surdutovich, Eur. Phys. J. D **60**, 1 (2010) DOI: 10.1140/epjd/e2010-00216-3
24. S. Ptasin´ska, S. Denif, P. Scheier, T.D. Mark, J. Chem. Phys. **120**, No. 18 8505 (2004)
25. K. Yong-Kim, M.E. Rudd, Phys. Rev. A. **50**, №5 3954 (1994) DOI: 10.1103/physreva.50.3954
26. I. Baccarelli, F.A. Gianturco, A. Grandi, N. Sanna, R.R. Lucchse, I. Bald, J. Kopyra, E. Illenberger, J. Am. Chem. Soc. **129**, 6269 (2007)
27. I. Baccarelli, N. Sanna, F.A. Gianturco, F. Sibasteanelli, J. Phys. Conf. Ser. **115**, 012009 (2008)
28. I. Chernyshova, E. Kontrosh, V. Roman, In contributed papers of the 32nd ICPEAC (virtual ICPEAC 2021, Canada) Book of Abstracts ViCPEAC 2021, July 20-23, 306 (2021)
29. I. Bald, J. Kopyra, E. Illenberger. Angew, Chem. Int. Ed. **45**, 4851 (2006). doi 10.1002/anie.200600303
30. O.B. Shpenik, A.M. Zavilopulo, A.S. Agafonova, L.G. Romanova, Rep. Nat. Acad. Sci. Ukraine №5, 96 (2008) http://dspace.nbuv.gov.ua/handle/123456789/4589
31. A.M. Zavilopulo, S.S. Demes, E.Yu. Remeta, A.I. Bulgakova, Ukr. J. Phys. **66**, 745 (2021) https://doi.org/10.15407/ujpe66.9.745*]*.
32. V.S. Vukstich, H.G. Bohachov, O.V. Vasiliev, E.Yu. Remeta, Ukr. J. Phys. **67**, 473 (2022) doi.org/10.15407/ujpe67.7.473
33. K. Yong-Ki, K.K. Irikura, M.A. Ali, J. Res. Nat. Inst. Stand. Technol. **105**, №2 285 (2000) DOI: 10.6028/jres.105.032
34. H. Tanaka, M.J. Brunger, L. Campbell, H. Kato, M. Hoshino, A.R.P. Rau, Rev. Mod. Phys. **88**, 025004 (2016) DOI: https://doi.org/10.1103/RevModPhys.88.025004
35. M. Gryzinski, Phys. Rev. **138** (2A), A336 (1965) doi.org/10.1103/PhysRev.138.A336.
36. S.S. Demes, O.V. Vasiliev, E.Yu. Remeta, Scient. Herald of Uzhhorod University. Series Physics. **47**, 101 (2020) doi.org/10.24144/2415-8038.2020.47.103-111.
37. Gaussian 09, Revision E.01. (Gaussian Inc., Wallingford CT. 2009)
38. M.C.A. Lopes, W.A.D. Pires, R.A.A. Amorim, A.C.P. Fernandes, T.M. Casagrande, D.B. Jones, F. Blanco, G. Garcia, M.J. Brunger, Intern. J. Mass Spectr. **456**, 116395 (2020) https://doi.org/10.1016/j.ijms.2020.116395
39. R.A.A. Amorim, A.C. Diniz, C.B. Oliveira, O.L. Oliveira Junior, D.B. Jones, F. Blanco, G. García, M.J. Brunger, M.C. A. Lopes, Eur. Phys. J. D **76**, 207 (2022)
40. NIST https://webbook.nist.gov/cgi/cbook.cgi
41. A.A. Radzig, B.M. Smirnov, *Reference Data on Atoms, Molecules and Ions* (Springer, Berlin, 1985)
42. R.T. Wiedmann, R.G. Tonkyn, M.G. White, K. Wang, V. McKoy, J. Chem. Phys. **97**, 768 (1992)
43. P. Erman, A. Karawajczyk, E. Rachlew-Kallne, C. Stromholm, J. Larsson, A. Persson, R. Zerne, Chem. Phys. Lett. **215**, 173 (1993)
44. J.M. Dyke, J. Chem. Soc. Faraday Trans. **83**, 69 (1987)
45. Y.-K. Kim, M.E. Rudd, Phys. Rev. A **50**, 3954 (1994)
46. Y.-K. Kim, J.-P. Desclaux, Phys. Rev. A **66**, 012708 (2002)
47. Y.-K. Kim, M.A. Alia, M.E. Rudd, J. Res. NIST **102**, 693 (1997)
48. W. Hwang, Y.-K. Kim, M.E. Rudd, J. Chem. Phys. **104**, 2956 (1996).
49. K.N. Joshipura, M. Vinodkumar, U.M. Patel, J. Phys. B: At. Mol. Opt. Phys. **34** 509 (2001)
50. Y.-K. Kim, K.K. Irikura, Proc. 2nd Int. Conf. On Atom. Molec. Data and Their Applications, ed. by K.A. Berrington, K.L. Bell, AIP Conf. Proc. (AIP, NewYork, NY) **543**, 220 (2000)
51. V. Tarnovsky, A. Leven, H. Deutsch, K. Becker, J. Phys. B**29**, 139 (1996)
52. F.A. Baiocchi, R.C. Wetzeland, R.S. Freund, Phys. Rev. Lett. **53**, 771 (1984)
53. D. Rapp, P. Englander-Golden, J. Chem. Phys. **43**, 1464 (1965)
54. O.J. Orient, S.K. Srivastava, J. Phys. B **20**, 3923 (1987)

55. M.B. Shah, D.S. Elliott, H.B. Gilbody, J. Phys B **20**, 3501 (1987)